2021 18th International Conference on Electrical Engineering, Computing Science and Automatic Control (CCE).
Mexico City, Mexico. November 10-12, 2021

Implementation of a BLDC Motor Observer Scheme using the INSTASPIN Platform

Axel Coronado
Instituto de Ingeniería
Univ. Nacional Autónoma de México
México City, México
acoronadoa@iingen.unam.mx

Alejandra de la Guerra
Univ. del Valle de México, Coyoacán
México City, México
alejandra_delaguerra@my.uvm.edu.mx
ORCID: 0000-0002-4700-6747

Luis Alvarez-Icaza
Instituto de Ingeniería
Univ. Nacional Autónoma de México
México City, México
ORCID: 0000-0001-9516-3950

***Abstract*—This article presents the application of the InstaSPIN-FOC™ solution by Texas Instruments to validate a disturbance observer for a permanent magnet brushless DC (BLDC) motor, providing experimental set-up and programming descriptions. Results compare the disturbance observer performance against the FAST observer included in the InstaSPIN-FOC™ and provide a guide to easily test other observer schemes.**

***Index Terms*—disturbance observer, BLDC motor, experimental platform**

I. Introduction

In recent years, the BLDC motor has become an alternative to DC and induction motors for variable speed drives given its simple structure, ruggedness, low cost, high efficiency, and speed versus torque characteristics. This in turn, makes this motor suitable for demanding applications such as Electric Vehicles as shown in [1]–[3].

Given the limitations of the Hall effect sensors normally used in BLDC motors, it is a common practice to design observer and estimation schemes aimed to recover continuos velocity and/or torque signals. This article presents the implementation of a disturbance observer for a High Voltage Brushless DC motor (BLDC) based on the InstaSPIN-FOC™ solution by Texas Instruments (TI).

The InstaSPIN-FOC™ is a sensorless Field Oriented Controller (FOC) by TI on-chip programmed in ROM on the TMS320F2806xF(M), TMS320F2802xF and TMS320F2805xF(M) device families. The system was designed to reduce cost and development time, while improving performance of three-phase variable speed motor systems. It includes the FAST observer, FOC, speed, and current loops [4]. The FAST observer is an Active Disturbance Rejection controller (ADRC) named after the estimated variables: Flux, Angle, Speed and Torque. The theory details behind this observer are explained in [5].

With respect to the use of this platform for experimental evaluation purposes, the work by [6] performs a comparison between the InstaSPIN and a standard industrial inverter for motors between 3-10 KW. The work in [5] also presents a comparison between the InstaSPIN and a PI controller in different applications settings. The results show that the InstaSPIN has a better performance with and without load. However, the industrial inverter has a graphical user interface which makes it easier to use than the InstaSPIN which must be programmed in C. Consequently, the work by [7], presents the design of a graphical user interface based on VisSim to solve the interface problem.

Additionally, the InstaSPIN Motor Control system has been widely used for rapid prototyping in applications such as: simulation model verification in [8], control platform testing in [9], development of parameter estimation system in [10], drone control in [11], robot control in [12], and velocity control for electric bicycles in [13].

A. FOC and observer description

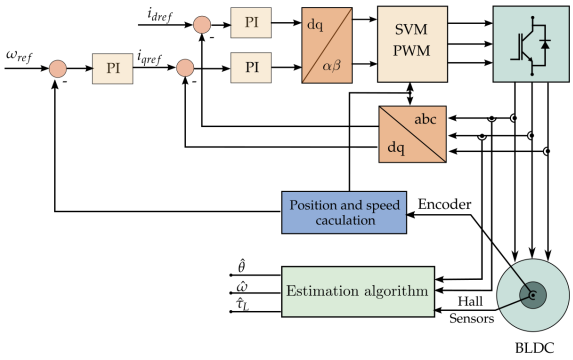

Fig. 1: Field oriented control and estimation algorithm.

Figure 1 shows a diagram of how the estimation algorithms and the field oriented control are implemented in the platform. The estimation algorithm is formed by a cascade connection of a linear observer and a differentiator presented in [14] by the authors. In the subsequent sections, this observer will be referenced as CLOD (Cascade Luenberger Observer with Differentiator). The objective of the CLOD is to estimate the angular velocity and to reconstruct a variable lumped disturbance in the rotor shaft of the motor, formed by the load torque and other dynamics not considered in the model. This is accomplished using the measurement of currents and discrete position information every 60 electrical degrees, obtained from Hall effect sensors. Also, it is assumed that the torque and its derivatives are bounded. If the above holds, the observer

978-1-6654-0029-9/21/$31.00 ©2021 IEEE

guarantees the convergence of the estimation error to zero in finite time in absence of noise, lectors are referred to [14] for more detail with respect to the CLOD design. As can be seen in Figure 1, the observer was tested in open loop.

With respect to the field oriented control in [15], the stator currents control is performed in the d-q reference frame of the rotor. Therefore, it is necessary to transform the measured currents from a three-phase static reference frame to a rotating d-q reference frame using the Park and Clark transformations represented as the abc-dq block in the Figure 1. The currents in the d-q reference frame are then controlled by PI controllers. The quadrature current is associated with the generation of torque, so the reference of the PI controller is the output of the PI speed controller. The reference for the direct current i_d, which is associated with the flux, is set to 0, since only the quadrature current produces useful torque. The voltages to be applied need to be transformed back to the three-phase reference frame of the stator from the d-q reference frame by using the inverse Park and Clark transformation. Before they can be used, these voltages are modulated using the space vector modulation technique (SVM), that calculates the periods of time in which certain states of the inverter, of the 8 possible states, need to be in order to obtain the average reference voltage. The objective of this work is to describe the implementation of an observer in the InstaSPIN experimental platform to show its potential as an easy and quick evaluation tool. In addition, some of advantages are mentioned and some disadvantages and its possible solution are bring up.

The article is organized as follows: Section II describes the experimental platform, Section III contains the microcontroller and the observer programming details, Section IV includes the results of the experimental evaluation and Section V presents the article conclusions.

II. Experimental platform

The brushless DC motor used was the BLY344S-240V-3000 from Anaheim Automation. This is a motor with star connected stator phases, sinusoidal back electro-motive force and four pair of poles whose parameters obtained from the data sheet [16] can be found in Table I. The BLDC motor has three Hall effect sensors placed at 120 electrical degrees between each other in the back of the motor, which are useful for a rough calculation of position and speed every 60 electrical degrees. In addition, an optical encoder with a resolution of 2000 pulses per revolution for a precise position and velocity calculation was connected to the motor shaft, whose signal is intended to be used as a means of comparison. The inverter used was the high voltage digital motor control and power factor correction kit (TMDSHVMTRPFCKIT) from TI. This board has a 3-phase inverter stage to control motors up to 350 [V] DC, an AC rectifier stage to generate the DC bus voltage for the inverter and isolated serial connectivity. Additionally, it is instrumented with three shunt resistors for current measurement of each stator phase. An aluminum base was built to mount the motor and encoder and, in addition, a 0.10 [m] radius aluminum flywheel with a mass of 0.372 [kg] was installed in the motor shaft as an inertial load. Figure 2 shows the complete experimental platform.

TABLE I: BLDC motor parameters

Parameter	Value
Rated Voltage	240 [V]
Rated Torque	2.1 [N m]
Rated Power	660 [W]
Resistance	1.2 [Ω]
Inductance	0.00475 [mH]
Electric constant	0.3455 [V/rad/s]
Mechanical constant	0.3811 [Nm/A]
Inertia	0.0002618 [kgm^2]
Viscous friction coefficient	0.000695 [Nms]

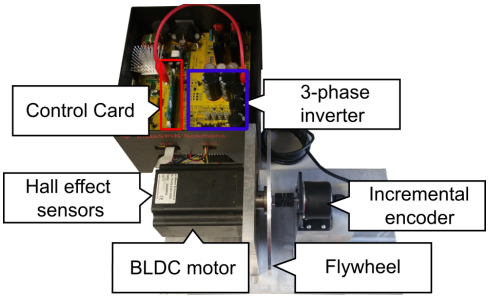

Fig. 2: Experimental platform.

III. Microcontroller and observer programming

The control board of the TMDSHVMTRPFCKIT is based on the low-cost micro controller F28069M Piccolo from TI. The TMS320F2806 is a high efficiency 32-bit CPU, with a floating point unit (FPU) capable of native single precision operations and a programmable control law accelerator which can execute code independently of the CPU. As already mention, the microcontroller has a built-in observer referred as FAST in the ROM. However, the observer design details are not described in the documentation and the code cannot be accessed. Nevertheless, the estimated torque by the FAST observer can be used to compare with the results of other observers, since at the moment, there is no torque sensor instrumented in the platform. Although the built-in estimator code is not accessible, the InstaSPIN-FOC™ documentation reports the commands to set the required inputs, get the outputs, and start the FAST observer, that requires the measurement of the phase voltages and currents as well as the knowledge of the motor parameters values (resistance, inductance, electrical constant, number of pair of poles, etc.) to function properly. Therefore, it has a starting routine where it estimates some of the above parameters. In addition to that, the gains for the current and speed PI controllers are calculated. These parameters, the limits of speed, current and voltage of the motor, as well as the offsets of the voltage and current sensors are logged in to a file, to be used later by the program. Originally, the programs were coded using the fixed point library IQmath because some microcontrollers compatible with the platform cannot

perform floating point operations. However, this library lacks some basic mathematical operators (such as the exponential) necessary for programming of the CLOD observer. For this reason and considering that the microcontroller used has a floating-point unit, the entire program as well as the estimation algorithms were rewritten using floating point. Before being programmed into the microcontroller, the CLOD observer first had to be discretized. In this case it was discretized using the backward Euler approximation. In this method, the derivatives in the state equations are replaced by the following expression:

$$\frac{dx}{dt} \approx \frac{x(k) - x(k-1)}{T_s} \tag{1}$$

where T_s is the sampling time.

As can be seen in the Figure 3, the code is divided into two parts: the part called *main ()* or main routine, initializes the driver, enables system interruptions and remains in an infinite loop until an interruption is detected. When the above happens, the main routine stops and the second part of the code, called *mainISR ()*, is executed. In this part, the source of the interruption is identified, the ADC ports, the encoder and the Hall effect sensors are read, the estimator algorithm is executed, and it is decided whether to run the current and speed PI controllers or not. The voltages obtained in the previous stage, before being applied to the motor, have to be modulated. This is done using the SVM technique which delivers the duty cycle to be written to the PWM ports. This ends the interrupt routine and execution returns to the infinite loop of the main routine, waiting for another interrupt. Specifically, the observer was tested in open loop with a sample time of $T_s = 1.33e^{-4}$ [s].

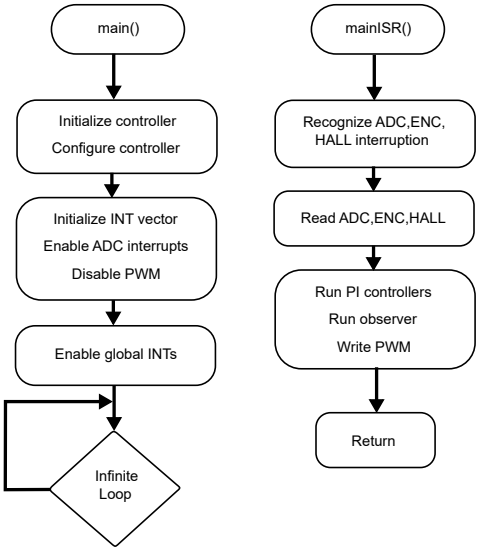

Fig. 3: Program flow chart.

IV. Experiments

This section presents the results of two experiments designed to show the behavior of the CLOD observer and the FAST observer with and without load torque.

The CLOD observer requires the load torque and its derivatives to be bounded, therefore it is necessary to generate sufficiently smooth speed trajectories. Hence, a smooth acceleration trajectory was designed and was later integrated to obtain the velocity trajectories used in the experiments.

The first test was performed without load torque. Figure 4a illustrates the behavior of the estimated angular velocity $\hat{\omega}$ by the CLOD observer, the estimated angular velocity $\hat{\omega}_F$ by the FAST observer and the measured velocity using the encoder ω_{enc} with Figure 4b showing the speed estimation error $e_\omega = \omega_{enc} - \hat{\omega}$. Figure 5 shows the estimated load torque $\hat{\tau_L}$ by the CLOD observer due to the rotor shaft inertia and the estimated load torque $\hat{\tau_{LF}}$ by the FAST observer.

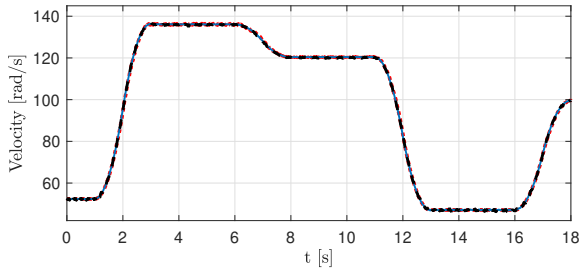

(a) Estimated velocity $\hat{\omega}$ (- - -), estimated velocity by FAST $\hat{\omega}_F$ (. . .) vs encoder velocity ω_{enc} (—)

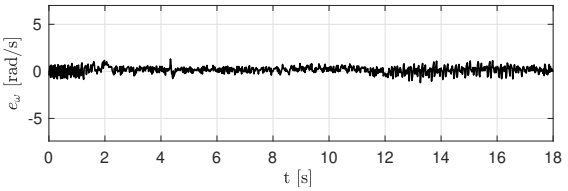

(b) Velocity estimation error.

Fig. 4: Experimental results without load: velocity estimation.

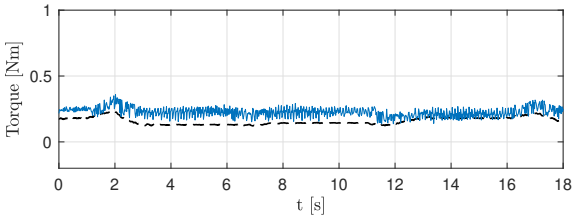

Fig. 5: Experimental results without load: estimated load torque $\hat{\tau}_L$ (- - -) vs estimated load torque by FAST $\hat{\tau}_{LF}$ (—).

In the second test, the flywheel was coupled to the motor shaft. The velocity reference was the same as in the previous test. Figure 6a illustrates the behavior of the estimated velocities $\hat{\omega}$, $\hat{\omega}_F$, compared with the measured velocity ω_{enc} and Figure 6b shows the velocity estimation error $e_\omega = \omega_{enc} - \hat{\omega}$. Figure 7 shows the estimated torques $\hat{\tau_L}$, $\hat{\tau_{FL}}$ due to the flywheel inertial load.

Despite the inertial load, both observers achieve a good estimate of the velocity, with an average error of less than 2% compared to ω_{enc}. Although the shape and magnitude

of the estimated torque by the observers is similar, an offset is observed. This offset may be caused by the different parameters used for the FAST ant the CLOD observers. In addition, the CLOD estimates the lumped load torque, that is, it estimates dynamics not considered in the model. Until there is a way to measure the load torque accurately, no conclusions can be made regarding the torque estimation error.

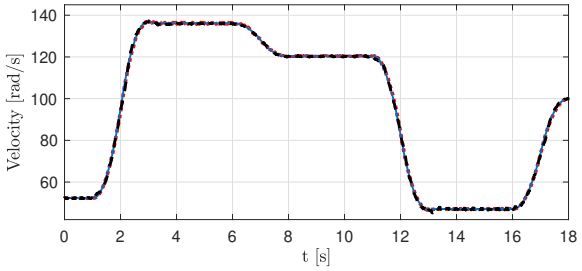

(a) Estimated velocity $\hat{\omega}$ (- - -), estimated velocity by FAST $\hat{\omega}_F$ (. . .) vs encoder velocity ω_{enc} (—)

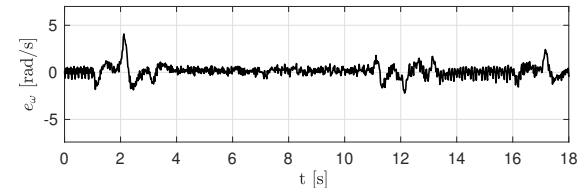

(b) Velocity estimation error.

Fig. 6: Experimental results with flywheel: velocity estimation.

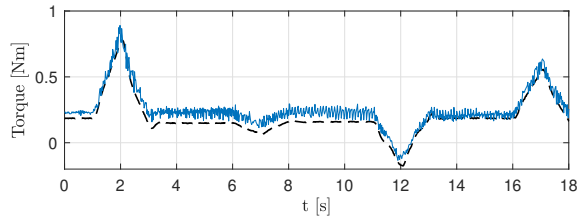

Fig. 7: Experimental results with flywheel: estimated load torque $\hat{\tau}_L$ (- - -) vs estimated load torque by FAST $\hat{\tau}_{LF}$ (—).

V. Conclusions

The results of the experiments show that the experimental platform is useful for testing different estimation algorithms with acceptable sampling time. The relative error in the speed estimation with the CLOD is less than 2% for speeds greater than 30 [rad/s] without load. In addition, it is possible to compare the magnitude and shape of the load torque, although not accurately, until a torque sensor is available. Therefore, the InstaSPIN-FOC™ platform is useful for observer validation using the TMS320F28069M microcontroller (which was previously owned). However, it is possible to achieve better performance by changing the microcontroller to be able to use smaller sample times. In addition, it was shown that the FAST observer results can be used as a quick, easy and economical way to compare disturbance observers. Finally, one possible drawback of the InstaSPIN-FOC™ solution is the fact that the platform must be programmed in C. This can be overcome by designing a friendly user interface as in [7]. Alternatively, the InstaSPIN-FOC™ platform can be connected to MATLAB/Simulink to have an easier interface for control design.

Acknowledgment

This work was supported by PAPITT grant IT101420. Axel Alejandro Coronado Andrade thanks CONACYT for support through scholarship CVU:856213. Authors declare that they have no conflict of interest.

References

[1] Mounir Zeraoulia, Mohamed El Hachemi Benbouzid, and Demba Diallo. Electric motor drive selection issues for hev propulsion systems: A comparative study. *IEEE Transactions Vehicle Technology*, 55(6):1756–1764, 2006.

[2] M. Ehsani, Y. Gao, S. Longo, and K. Ebrahim. *Modern electric, hybrid electric, and fuel cell vehicles*. CRC press, 2018.

[3] Tahir Aja Zarma, Ahmadu Adamu Galadima, and Maruf A Aminu. Review of motors for electrical vehicles. *Journal of Scientific Research and Reports*, pages 1–6, 2019.

[4] Texas Instruments. InstaSPIN-FOC and InstaSPIN-MOTION User's Guide. *Literature Number: SPRUHJ1A*, 2013.

[5] Qing Zheng and Zhiqiang Gao. Active disturbance rejection control: some recent experimental and industrial case studies. *Control Theory and Technology*, 16(4):301–313, 2018.

[6] Matthias Blank, Philipp Löhdefink, Benjamin Reinhardt, and Armin Dietz. Evaluation of a new microcontroller based solution for sensorless control of electrical drives. In *2014 6th European Embedded Design in Education and Research Conference (EDERC)*, pages 132–136. IEEE, 2014.

[7] Vardi Satya Kumari, Syed Sarfaraz Nawaz, et al. Speed control of BLDC motor using DRV8312EVM in VisSim Environment. *CVR Journal of Science and Technology*, 14:43–48, 2018.

[8] Udai Shipurkar, Tim D Strous, Henk Polinder, JA Ferreira, and André Veltman. Achieving sensorless control for the brushless doubly fed induction machine. *IEEE Transactions on Energy Conversion*, 32(4):1611–1619, 2017.

[9] Mohd Afroz Akhtar, Md Musraph Hussain, Partha Sarathi Pal, and Suman Saha. dSPACE based motor testing platform for characterization of BLDC Motor performance under different loading conditions. In *2018 8th IEEE India International Conference on Power Electronics (IICPE)*, pages 1–6. IEEE, 2018.

[10] Claudiu-Ionel Nicola, Marcel Nicola, Adrian Vintilă, and Dumitru Sacerdoţianu. Identification and sensorless control of PMSM using FOC strategy and implementation in embedded system. In *2019 International Conference on Electromechanical and Energy Systems (SIELMEN)*, pages 1–6. IEEE, 2019.

[11] Kristen N Mogensen. Motor-control considerations for electronic speed control in drones. *Analog Applications Journal [online]. Texas Instruments*, 2016.

[12] Ankit Bhatia, Aaron M Johnson, and Matthew T Mason. Direct drive hands: Force-motion transparency in gripper design. In *Robotics: science and systems*, 2019.

[13] David Florez, Henry Carrillo, Ricardo Gonzalez, Max Herrera, Ronald Hurtado-Velasco, Martha Cano, Sergio Roa, and Tatiana Manrique. Development of a Bike-Sharing system based on pedal-assisted electric bicycles for Bogota City. *Electronics*, 7(11), 2018.

[14] Axel Coronado Andrade, Alejandra de la Guerra, and Luis Alvarez Icaza. Observador en cascada para la estimación del par de carga en un motor de cd sin escobillas. In *Congreso Nacional de Control Automático 2019*, pages 582–587, Puebla, Puebla, México, 2019. AMCA.

[15] Joseph P John, S. Suresh Kumar, and B. Jaya. Space vector modulation based field oriented control scheme for brushless dc motors. *2011 International Conference on Emerging Trends in Electrical and Computer Technology*, 2011.

[16] Anaheim Automation. BLY34 Series - Brushless DC Motors, 2021.